DO EINSTEIN'S EQUATIONS DESCRIBE REALITY WELL?

*M. Křížek**

Dedicated to Dr. Milan Práger on his 90th birthday.

Abstract: The standard cosmological model that is based on Einstein's equations possesses many paradoxes. Therefore, we take a closer look at the equations themselves, and not only on cosmological scales. In this survey paper, we present 10 significant problems and drawbacks of Einstein's equations investigated by the author. They include their extremely large complexity, non-differentiability of the metric, difficulties with initial and boundary conditions, multiple divisions by zero, excessive extrapolations to cosmological distances leading to mysterious dark matter and dark energy entities, unconvincing relativistic tests, the absence of aberration effects, and scale non-invariance. We also discuss a slight violation of the laws of conservation of energy and of momentum.

This paper is a natural continuation of paper [36] about the criticism of the standard cosmological model that is based on Einstein's equations. Albert Einstein derived these equations more than 100 years ago and their agreement with the reality seemed to be very good that time.

Later, new measurement methods and devices were invented in cosmology that provide more accurate data and also completely new approaches to the study of some physical phenomena. This progress in cosmological measurements and new mathematical models for some parts of the physical model have brought the possibility to compare Einstein's original equations with this new development. We present 10 substantial drawbacks of Einstein's equations that have been discovered in this process of comparison. Their origin often lies in the limited precision of measured data, identifying mathematical models with reality [38], and their incorrect interpretations. For example, Einstein's equations imply the well-known Friedmann equation describing the expansion of a homogeneous and isotropic universe. It is an autonomous ordinary differential equation with constant coefficients. However, from such a simple and trivial equation far-reaching conclusion about the deep past and the far future are made. Other categorical conclusions include the

---

*Michal Křížek; Institute of Mathematics, Czech Academy of Sciences, Žitná 25, CZ-115 67 Prague 1, Czech Republic, E-mail: krizek@math.cas.cz

existence of dark matter and dark energy and the age of the universe 13.79 Gyr up to four significant digits [52].

Further problems arise from the nonlinearity and instability of Einstein's equations, division by zero, subtraction of two inexact numbers of almost the same size. This usually leads to a catastrophic loss of accuracy [7]. Finally note that many conclusions in cosmology are not in the form of mathematical implications, since various simplifications and approximations are done.

1.   Extreme complexity of Einstein's equations

In November 1915, Albert Einstein [17] (see also [18]) introduced his field equations of general relativity consisting of 10 equations

$$R_{\mu\nu} - \frac{1}{2} R g_{\mu\nu} = \frac{8\pi G}{c^4} T_{\mu\nu}, \quad \mu, \nu = 0, 1, 2, 3, \tag{1}$$

of the unknown 4×4 symmetric metric tensor $g_{\mu\nu}$ of one timelike variable x^0 and three Cartesian or curvilinear space variables x^1, x^2, x^3, i.e. $g_{\mu\nu} = g_{\mu\nu}(x^0, x^1, x^2, x^3)$ (for simplicity the dependence of all functions from Eq. (1) on these variables will be nowhere indicated), where

$$R_{\mu\nu} = \sum_{\varkappa=0}^{3} R^{\varkappa}_{\mu\varkappa\nu} \tag{2}$$

is the 4×4 symmetric *Ricci tensor*,

$$R = \sum_{\mu,\nu=0}^{3} g^{\mu\nu} R_{\mu\nu} \tag{3}$$

is the *Ricci scalar* (i.e. the scalar curvature), $G = 6.674 \cdot 10^{-11} \text{ m}^3\text{kg}^{-1}\text{s}^{-2}$ is the gravitational constant, $c = 299\,792\,458$ m/s is the speed of light in vacuum (the constant $8\pi G/c^4$ does not appear in [17], since Einstein did not use SI units), $T_{\mu\nu}$ is the 4×4 symmetric *tensor of density of energy and momentum*,

$$R^{\varkappa}_{\mu\sigma\nu} = \frac{\partial \Gamma^{\varkappa}_{\mu\nu}}{\partial x^\sigma} - \frac{\partial \Gamma^{\varkappa}_{\mu\sigma}}{\partial x^\nu} + \sum_{\lambda=0}^{3} \Gamma^{\lambda}_{\mu\nu} \Gamma^{\varkappa}_{\lambda\sigma} - \sum_{\lambda=0}^{3} \Gamma^{\lambda}_{\mu\sigma} \Gamma^{\varkappa}_{\lambda\nu} \tag{4}$$

is the *Riemann curvature tensor* that has 20 independent components from $4^4 = 256$ components due to several symmetries[1], where

$$\Gamma^{\mu}_{\varkappa\sigma} = \frac{1}{2} \sum_{\nu=0}^{3} g^{\mu\nu} \left(\frac{\partial g_{\varkappa\nu}}{\partial x^\sigma} + \frac{\partial g_{\sigma\nu}}{\partial x^\varkappa} - \frac{\partial g_{\varkappa\sigma}}{\partial x^\nu} \right) \tag{5}$$

are *Christoffel's symbols of the second kind* (also called the *connection coefficients*) and all derivatives are supposed to be classical. From this and the relation $g_{\varkappa\sigma} =$

---

[1]In any space dimension N the Riemann curvature tensor has $N^2(N^2 - 1)/12$ independent entries due to the following conditions: $R^{\varkappa}_{\mu\sigma\nu} + R^{\varkappa}_{\sigma\nu\mu} + R^{\varkappa}_{\nu\mu\sigma} = 0$ (the *First Bianchi identity*) and $R_{\lambda\mu\sigma\nu} = -R_{\mu\lambda\sigma\nu} = -R_{\lambda\mu\nu\sigma}$, where $R_{\lambda\mu\sigma\nu} = \sum_{\varkappa} g_{\lambda\varkappa} R^{\varkappa}_{\mu\sigma\nu}$. Thus, $R_{\lambda\mu\sigma\nu} = R_{\sigma\nu\lambda\mu}$.

$g_{\sigma\varkappa}$ one can derive the symmetry $\Gamma^{\mu}_{\ \varkappa\sigma} = \Gamma^{\mu}_{\ \sigma\varkappa}$ for $\mu = 0, 1, 2, 3$ (see Eq. (41) and Eq. (46) for the proof). Thus altogether we have $40 = 4 \times (1+2+3+4)$ independent components. Finally, $g^{\mu\nu}$ is the 4×4 symmetric matrix inverse to $g_{\mu\nu}$, i.e.

$$g^{\mu\nu} = \frac{g^{*}_{\mu\nu}}{\det(g_{\mu\nu})}, \qquad \det(g_{\mu\nu}) = \sum_{\pi \in S_4} (-1)^{\operatorname{sgn}\pi} g_{0\nu_0} g_{1\nu_1} g_{2\nu_2} g_{3\nu_3},$$

where the entries $g^{*}_{\mu\nu}$ form the 4×4 matrix of 3×3 algebraic adjoints of $g_{\mu\nu}$, S_4 is the symmetric group of 24 permutations π of indices $(\nu_0, \nu_1, \nu_2, \nu_3)$, $\operatorname{sgn}\pi = 0$ for an even permutation and $\operatorname{sgn}\pi = 1$ for an odd permutation.

Making all the above substitutions, the explicit expressing of the left-hand side of Eq. (1) would occupy many pages with thousands of terms (partial derivatives of real functions).[2] For comparison note that the Laplace equation $\Delta u = 0$ has only three terms $\partial^2 u / \partial x_i^2$ on its left-hand side, $i = 1, 2, 3$, and the famous Navier-Stokes equations 24 terms.

Working with curved spacetime, one necessarily faces the extreme complexity of the nonlinear system of second order partial differential Einstein's equations (1). It is so complicated that we do not know any of its analytical solutions for two or more massive bodies (cf. [44]). Furthermore, there are no suitable guaranteed error estimates for numerical solutions. Thus a natural question arises whether Einstein's equations describe reality sufficiently accurately. Their general form Eq. (1) has not been tested, yet.

2. Non-differentiability of the Schwarzschild metric

In Eq. (1), we shall first assume that

$$T_{\mu\nu} = 0. \tag{6}$$

From now on we shall use the standard *Einstein summation convention* for summation over repeating upper and lower index. Multiplying Eq. (1) by $g^{\mu\nu}$, we find by Eqs. (3) and (6) that

$$0 = g^{\mu\nu} R_{\mu\nu} - \frac{1}{2} R g^{\mu\nu} g_{\mu\nu} = R - \frac{1}{2} R \delta^{\mu}_{\ \mu} = R - 2R, \tag{7}$$

where $\delta^{\mu}_{\ \nu}$ is the Kronecker delta and

$$\delta^{\mu}_{\ \mu} = 4.$$

Hence, $R = 0$ and Einstein's equations (1) with right-hand side Eq. (6) can be rewritten as

$$R_{\mu\nu} = 0, \tag{8}$$

where by Eqs. (2) and (4)

$$R_{\mu\nu} = \Gamma^{\varkappa}_{\ \mu\nu,\varkappa} - \Gamma^{\varkappa}_{\ \mu\varkappa,\nu} + \Gamma^{\lambda}_{\ \mu\nu}\Gamma^{\varkappa}_{\ \lambda\varkappa} - \Gamma^{\lambda}_{\ \mu\varkappa}\Gamma^{\varkappa}_{\ \nu\lambda}. \tag{9}$$

---

[2] In spite of that in [44, p. 42] one can read: *No equation of physics can be written more simply.*

Here the index after the comma indicates the ordered number of a variable with respect to which we differentiate, i.e. $\Gamma^{\varkappa}_{\mu\nu,\varkappa} = \partial\Gamma^{\varkappa}_{\mu\nu}/\partial x^{\varkappa}$.

Einstein himself did not believe that somebody will ever find a solution of Eq. (1). However, already on December 22, 1915, Karl Schwarzschild wrote to Albert Einstein that he has found a solution [57] (for the English translation of Schwarzschild's original letter by R. A. Rydin see [16]). The Schwarzschild solution of Eq. (8) can be written as the following diagonal tensor

$$g_{\mu\mu} = \text{diag}\left(-\frac{r-S}{r}, \frac{r}{r-S}, r^2\sin^2\theta, r^2\right), \tag{10}$$

$g_{\mu\nu} = 0$ for $\mu \neq \nu$, where the line element satisfies

$$ds^2 = -\frac{r-S}{r}c^2 dt^2 + \frac{r}{r-S}\,dr^2 + r^2\sin^2\theta\,d\varphi^2 + r^2 d\theta^2, \tag{11}$$

$r > S$, the constant S is given by Eq. (12) below, t is a time coordinate, (r,φ,θ) are the standard spherical coordinates, $\varphi \in [0, 2\pi)$, $\theta \in [0,\pi]$, i.e. $x^0 = ct$, $x^1 = r\sin\theta\cos\varphi$, $x^2 = r\sin\theta\sin\varphi$, and $x^3 = r\cos\theta$.

Schwarzschild assumed that the gravitational field has the following properties:
(a) it is static,
(b) it is spherically symmetric,
(c) the spacetime is empty,
(d) the spacetime is asymptotically flat.

For a fixed nonrotating ball in vacuum with mass $M > 0$ and with a spherically symmetric mass distribution we set

$$S = \frac{2MG}{c^2} \tag{12}$$

which is called the *Schwarzschild gravitational radius*. From this we see that the metric Eq. (10) changes into the standard Minkowski (pseudo)metric for $M \to 0$. According to well-known Birkhoff's theorem (see [4]), the space outside a ball with spherically symmetric mass distribution is described by Eq. (10) which is called the *exterior Schwarzschild metric*, see e.g. [41], [44], [45].

In Appendices A and B, we show in detail that the classical Schwarzschild solution Eq. (10) satisfies Eq. (1) with zero right-hand side Eq. (6). The reason for this exposition is that everyone can recalculate some important formulae used in subsequent sections. Another reason is that classical tests of general relativity are usually based just on the exterior Schwarzschild solution.

In 1916 Karl Schwarzschild (see [58]) found the first nonvacuum solution of Einstein's equation (1). He assumed that the ball with coordinate radius $r_0 > 0$ is formed by an ideal incompressible non-rotating fluid with constant density to avoid a possible internal mechanical stress that may have a non-negligible influence on the resulting gravitational field. He also assumed the zero pressure at the surface. Then (see e.g. [21], [23, p. 529], [60, p. 213]) the corresponding metric is

$$g_{\mu\mu} = \text{diag}\left(-\frac{1}{4}\left(3\sqrt{1-\frac{S}{r_0}} - \sqrt{1-\frac{Sr^2}{r_0^3}}\right)^2, \frac{r_0^3}{r_0^3 - Sr^2}, r^2\sin^2\theta, r^2\right), \tag{13}$$

where $r \in [0, r_0]$ and S is given by Eq. (12). The corresponding metric tensor is called the *interior Schwarzschild solution*, see [60, p. 213]. It is again a static solution, meaning that it does not change over time. To avoid the division by zero in the component g_{11}, we require

$$\frac{r_0^3}{r_0^3 - Sr^2} = \left(1 - \frac{Sr^2}{r_0^3}\right)^{-1} > 0 \quad \text{for all } r \in [0, r_0]$$

which leads to the inequality

$$r_0 > S. \tag{14}$$

Note that the ball in question is not a black hole and Eq. (13) is not a black hole metric. Using Eq. (10) and (13), we can easily verify that the exterior and interior metric have the same values for $r = r_0$, i.e., each component $g_{\mu\mu} = g_{\mu\mu}(r)$ is a continuous function on $[0, \infty)$ for $\mu = 0, 1, 2, 3$.

By inspection we can also find that g_{00}, g_{22}, and g_{33} are smooth functions at $r = r_0$ (i.e., their first derivatives are continuous). However, now we will show that the first derivatives of g_{11} of the exterior and interior Schwarzschild solution do not match (see Fig. 1). The reason is that they have a jump on the common boundary $r = r_0$, even though the 2nd order Einstein's equations contain classical derivatives of $g_{\mu\nu}$ which are supposed to be continuous in definition Eq. (5). Therefore, the corresponding space manifold described by the Riemann curvature tensor is not differentiable, since the tangent hyperplane for $r = r_0$ cannot be uniquely defined. All Riemannian manifolds must be locally flat which is not true in this particular case, i.e., the geometry of the corresponding spacetime must be everywhere locally Lorentzian [44, p. 29].
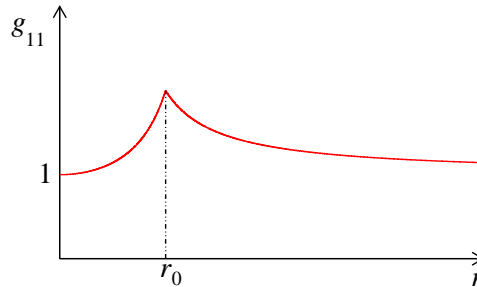

Fig. 1 *The behavior of the non-differentiable component $g_{11} = g_{11}(r)$ of the metric tensor from Eq. (10) and (13). The first derivative $(\partial g_{11}/\partial r)(r_0)$ is not defined. The piecewise rational function g_{11} cannot be smoothed near r_0, since then Einstein's equations (1) would not be valid in a close neighborhood of r_0.*

We observe that the corresponding boundary conditions

$$\frac{\partial g_{11}}{\partial r}(0) = 0 \quad \text{and} \quad g_{11}(r) \to 1 \text{ for } r \to \infty$$

are quite natural due to spherical symmetry. From Eq. (10) we see that the one-sided limit from above of the component $g_{11}(r) = r/(r - S)$ of the exterior solution

is negative

$$\lim_{r \to r_0^+} \frac{\partial g_{11}}{\partial r}(r) < 0,$$

whereas the component $g_{11}(r)$ of the interior solution Eq. (13) is an increasing function on $[0, r_0]$ (cf. Fig. 1). It is increasing even for a variable spherically symmetric density. Consequently, Eq. (1) cannot be used inside the ball with radius $r_1 > r_0$ to model our Sun or any other star with radius r_0 together with its spherically symmetric vacuum neighborhood (see Fig. 2 and Eq. (5)). This is a serious drawback of Einstein's equations, since the composite metric tensor Eq. (10)+(13) is not differentiable for $r = r_0$. For a different choice of coordinates (e.g. Kruskal-Szekeres like coordinates) the corresponding manifold remains non-differentiable. Consequently, Eq. (10) and (13) are only local solutions and together they do not form a global solution[3] of Einstein's equations inside the ball with radius r_1. The jump in the first derivative of g_{11} will appear even if we slightly deviate from spherical symmetry, since local solutions continuously depend on data.

Let us emphasize that the covariant divergence of the right-hand side of Eq. (1) has to be zero, see Eq. (38) below. Therefore, the covariant divergence of the left-hand side is zero, too. However, this requires further differentiation of the non-differentiable metric tensor at r_0.
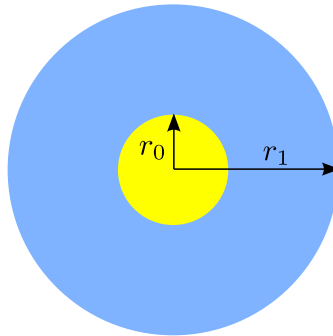

Fig. 2 *A schematic illustration of the Sun with its spherically symmetric neighborhood.*

For comparison, note that the first classical derivatives of the Newton potential u of a similar problem are continuous. It is described by the Poisson equation $\Delta u = 4\pi G\rho$, where ρ is the mass density. Let the right-hand $f = 4\pi G\rho$ side be spherically symmetric and such that $f(r) = 1$ for $r \in [0, 1]$ and $f(r) = 0$ otherwise. Its solution is $u(r) = \frac{1}{6}r^2 - \frac{1}{2}$ for $r \in [0, 1]$ and $u(r) = -1/(3r)$ otherwise. Hence, both u and $\partial u/\partial r$ are continuous at $r_0 = 1$.

---

[3]Similarly, the function $u(x) = |x|$ is a local classical solution of the second order ordinary differential equation $u'' = 0$ on the intervals $[-1, 0]$ and $[0, 1]$, but it is not a global solution over the interval $[-1, 1]$. It is not even a weak or very weak solution there.

3. Difficulties with initial and boundary conditions

Einstein's equations (1) without initial and boundary conditions may have more different solutions (see e.g. Theorem 1 below). Since Eq. (1) represents a system of hyperbolic equations with second time derivatives, two initial conditions should be prescribed. These equations are highly nonlinear. Therefore, the existence and uniqueness of a weak solution of Einstein's equations with some initial and boundary conditions is a serious problem. Note, for example, that the one-dimensional steady-state nonlinear heat conduction equations with any type of boundary conditions does not have a unique weak solution even when the heat conduction coefficient is continuous, see [26, p. 182].

It is usually difficult, if not impossible, to prescribe explicitly any appropriate initial and boundary conditions for non-spherically symmetric regions for $g_{\mu\nu}$ satisfying Eq. (1). The reason is that matter tells spacetime how to curve and spacetime tells matter how to move. So the initial space manifold is a priori not known except for some special cases when the analytical solution of Einstein's equation is known. More precisely, the left-hand side of Eq. (1) corresponds to geometry and the *Einstein tensor* $G_{\mu\nu} := R_{\mu\nu} - \frac{1}{2}Rg_{\mu\nu}$ tells gravitational spacetime how to curve. The right-hand side of Eq. (1) corresponds to physics and the tensor $T_{\mu\nu}$ tells matter how to move.

Furthermore, let us point out that the knowledge of the metric tensor $g_{\mu\nu}$ does not determine the topology of the corresponding manifold. For instance, the Euclidean space $\mathbb{E}^3$ has the same metric as $\mathbb{S}^1 \times \mathbb{E}^2$, but different topology. Here $\mathbb{S}^1$ stands for the unit circle. Other examples can be found in [44, p. 725].

In 1917, Albert Einstein introduced a new form of his equations (see [19])

$$R_{\mu\nu} - \frac{1}{2}Rg_{\mu\nu} + \Lambda g_{\mu\nu} = \frac{8\pi G}{c^4}T_{\mu\nu} \tag{15}$$

with non-zero cosmological constant Λ to avoid a gravitational collapse of the whole universe. It is said that the gravitational constant G is the worst established constant of all fundamental physical constants, since its value is known only to 3 (or 4) significant digits. However, we do not know any significant digit of the cosmological constant Λ, yet. Note that the standard cosmological model only assumes that $\Lambda \approx 10^{-52}$ m^{-2}.

Theorem 1. *Let $g_{\mu\nu}$ be a solution of Eq. (15). Then $(-g_{\mu\nu})$ solves Eq. (15) if we replace Λ by $(-\Lambda)$. In particular, if $\Lambda = 0$, then $(-g_{\mu\nu})$ solves Eq. (1).*

Proof. Using Eq. (5), we observe that the Christoffel's symbols remain the same if we replace $g_{\mu\nu}$ by $(-g_{\mu\nu})$, namely,

$$\Gamma^{\mu}_{\varkappa\sigma} = \frac{1}{2}(-g^{\mu\nu})\Big(-\frac{\partial g_{\varkappa\nu}}{\partial x^{\sigma}} - \frac{\partial g_{\sigma\nu}}{\partial x^{\varkappa}} + \frac{\partial g_{\varkappa\sigma}}{\partial x^{\nu}}\Big).$$

By Eq. (2) and (4) we find that the Ricci tensor $R_{\mu\nu}$ in Eq. (15) does not change as well. Concerning the second term on the left-hand side of Eq. (15), we see from Eq. (3) that $(-\frac{1}{2}Rg_{\mu\nu})$ remains also unchanged if we replace $g_{\mu\nu}$ by $(-g_{\mu\nu})$. Finally, for the third term we get $\Lambda g_{\mu\nu} = -\Lambda(-g_{\mu\nu})$. $\square$

Finally emphasize that Einstein's equations are fully deterministic whereas the universe does not operate solely gravitationally due to quantum phenomena. Their

effects can be observed not only on microscopic scales. For instance, we may decide whenever we wish to change the trajectory of an asteroid in arbitrary direction by the famous kinetic impactor method. The evolution of the real world is thus probably unstable with respect to initial conditions, since small quantum fluctuations can produce big consequences. Such processes cannot be described by Einstein's equations.

4. Division by zero in the Schwarzschild-de Sitter model

Let us seek a solution of Eq. (15) when

$$T_{\mu\nu} = 0.$$

Similarly as in Eq. (7) we find by Eq. (3) that

$$0 = g^{\mu\nu}R_{\mu\nu} + \left(\Lambda - \tfrac{1}{2}R\right)g^{\mu\nu}g_{\mu\nu} = R + 4\left(\Lambda - \tfrac{1}{2}R\right) = 4\Lambda - R,$$

i.e., in this case Einstein's equation (15) can be rewritten as

$$R_{\mu\nu} = \Lambda g_{\mu\nu}. \tag{16}$$

When Einstein's paper [19] appeared, then afterwards several articles (cf. [27, p. 438], [68]) were published that looked for an exterior Schwarzschild-like solution of Eq. (16) using the standard spherical coordinates, see Appendix C,

$$g_{\mu\mu} = \operatorname{diag}\left(-\left(\frac{r-S}{r} - \frac{\Lambda r^2}{3}\right), \left(\frac{r-S}{r} - \frac{\Lambda r^2}{3}\right)^{-1}, r^2 \sin^2\theta, r^2\right), \tag{17}$$

where S is given by Eq. (12), $r > S$, and $\theta \in [0, \pi]$. We observe that Eq. (17) reduces to the exterior Schwarzschild metric (10) for $\Lambda = 0$. If $\Lambda \neq 0$ and $S = 0$ (i.e., $M = 0$ by Eq. (12)), we get the de Sitter or anti-de Sitter metric [14]. Moreover, if $\Lambda = 0$ and $S = 0$ then Eq. (17) changes into the Minkowski metric.

For $\Lambda > 0$ and

$$L := \Lambda^{-1/2} \tag{18}$$

let $S > 0$ be such that $S < L/2$. Then

$$g_{00}(L) = -1 + \frac{S}{L} + \frac{1}{3} < -\frac{2}{3} + \frac{L}{2L} < 0, \quad g_{00}(2L) = -1 + \frac{S}{2L} + \frac{4\Lambda L^2}{3} = \frac{1}{3} + \frac{S}{2L} > 0. \tag{19}$$

Hence, the continuous component $g_{00} = g_{00}(r)$ changes its sign on the interval $(L, 2L)$, i.e., there exists $\bar{r} \in (L, 2L)$ such that $g_{00}(\bar{r}) = 0$. Consequently, in the evaluation of the next component

$$g_{11}(r) = \left(\frac{r-S}{r} - \frac{\Lambda r^2}{3}\right)^{-1}$$

one divides by zero for $r = \bar{r}$ and the metric breaks down. The metric tensor Eq. (17) is thus not well defined at cosmological distances even though the cosmological constant was invented just to treat extremely large distances in the universe.

The component $g_{11}(r)$ attains arbitrarily large values when $r \to \bar{r}^{-}$ even though there is no physical barrier. Therefore, the quadratic form $g_{\mu\nu}(r)v^{\mu}v^{\nu}$ is also not well-defined at $r = \bar{r}$ for any contravariant vector v^{μ} such that $v^1 \neq 0$. A different choice of coordinates does not help to avoid this singularity, since the form does not change its value for any given r.

5. Division by zero in the Friedmann model

We meet division by zero also for a nonzero right-hand side of Eq. (15). In cosmology, the metric of the expanding homogeneous and isotropic universe is expressed by the *Robertson–Walker metric*

$$\mathrm{d}s^2 = -c^2\mathrm{d}t^2 + a^2(t)\big(\mathrm{d}\chi^2 + \mathrm{sinn}^2\chi(\mathrm{d}\theta^2 + \sin^2\theta\,\mathrm{d}\varphi^2)\big)$$

(see e.g. [41], [44]), where $\theta \in [0, \pi]$, $\varphi \in [0, 2\pi)$, $\chi \in [0, \pi]$ for $k = 1$ and $\chi \in [0, \infty)$ otherwise, χ is a dimensionless *comoving distance*, $a = a(t)$ is a smooth positive function which is called the *expansion function*, and sinn depends on the curvature index $k \in \{-1, 0, 1\}$ as follows

$$\mathrm{sinn}\,\chi = \begin{cases} \sin\chi & \text{if } k = 1, \\ \chi & \text{if } k = 0, \\ \sinh\chi & \text{if } k = -1. \end{cases} \tag{20}$$

The corresponding metric tensor is then given by the diagonal matrix

$$g_{\mu\mu} = \mathrm{diag}(-1, a^2, a^2\mathrm{sinn}^2\chi, a^2\mathrm{sinn}^2\chi\sin^2\theta), \quad \mu = 0, 1, 2, 3.$$

If $k = 1$ then $a(t)$ is the radius of the space represented by the three-dimensional sphere $\mathbb{S}^3(t)$.

We shall assume that $a = a(t)$ satisfies the *Friedmann ordinary differential equation*

$$\dot{a}^2 = \frac{8\pi G\rho a^2}{3} + \frac{\Lambda c^2 a^2}{3} - kc^2 \tag{21}$$

for $t > \tau$, where the dot denotes the time derivative, $\rho = \rho(t) > 0$ is the mean mass density, and

$$\tau \approx 380\,000 \text{ yr}$$

is the time of decoupling of the cosmic microwave background radiation (cf. Eq. (26) and the footnote 5 below). In [25] Alexander Friedmann derived Eq. (21) exactly from Eq. (15) without any approximations, i.e., Eq. (21) is a direct mathematical consequence of Eq. (15) for a homogeneous and isotropic expanding universe, see [34] for the proof.

We shall suppose that

$$\dot{a}(\tau) > 0, \tag{22}$$

since the universe was expanding at time τ. Furthermore, assume that $\dot{a}(t) \neq 0$ for all $t > \tau$ and divide equation Eq. (21) by $\dot{a}^2$. Then the Friedmann equation reads

$$\Omega_{\mathrm{M}}(t) + \Omega_{\Lambda}(t) + \Omega_k(t) = 1 \quad \text{for all } t > \tau, \tag{23}$$

where

$$\Omega_{\mathrm{M}}(t) = \frac{8\pi G \rho(t)}{3H^2(t)} > 0, \quad \Omega_\Lambda(t) = \frac{\Lambda c^2}{3H^2(t)}, \quad \text{and} \quad \Omega_k(t) = -\frac{kc^2}{a^2(t)H^2(t)}, \quad (24)$$

are normalized cosmological parameters called (see [49, p. 58], [52, p. 37]) the *density of dark and baryonic matter, density of dark energy,* and the *curvature parameter,* respectively, and

$$H(t) = \frac{\dot{a}(t)}{a(t)}$$

is the *Hubble parameter.* Note that Eq. (23) is really a differential equation, since the derivative $\dot{a}$ is hidden in the Hubble parameter.

In the literature on cosmology, the division of Eq. (21) by the square $\dot{a}^2 \geq 0$ is usually done without any preliminary warning that we may possibly divide by zero which may lead to various paradoxes. For instance, we see by Eq. (24) that

$$\dot{a}(t) \to 0 \quad \Longrightarrow \quad \Omega_{\mathrm{M}}(t) \to \infty \quad \text{and} \quad \Omega_\Lambda(t) \to \pm\infty \quad \text{for} \quad \Lambda \neq 0, \quad (25)$$

corresponding e.g. to an oscillating universe or the Einstein static[4] but unstable solution $a(t) \equiv \Lambda^{-1/2}$ for $\Lambda > 0$ (cf. Eq. (18)) or de Sitter solution $a(t) = \alpha \cosh(ct/\alpha)$ for $\rho = 0$ and a suitable constant $\alpha > 0$ (see e.g. [12], [14], [19], [40]). Is there really an infinite density of dark matter and dark energy, when $a = a(t)$ reaches its extremal values? The true density of baryonic matter is surely finite.

Now we show that division by zero in Eq. (24) may appear for Λ negative, vanishing, and also positive. Setting

$$A = \frac{\Lambda c^2}{3} \quad \text{and} \quad B = -kc^2,$$

the Friedmann equation (21) can be rewritten as the following simple autonomous ordinary differential equation with constant coefficients[5]

$$\dot{a}^2 = Aa^2 + B + \frac{C}{a} \quad \text{for } t \geq \tau, \quad (26)$$

where $C = 8\pi G \rho a^3 / 3 > 0$ is constant by the law of conservation of mass for zero pressure, i.e. $\rho(t)a^3(t) = \rho(t_0)a^3(t_0)$, where t_0 is the present time (see [35, p. 100]). If $\dot{a} \not\equiv 0$ then by Eq. (26) we can find that

$$\ddot{a}(t) = Aa(t) - \frac{C}{2a^2(t)}. \quad (27)$$

1) First assume that $\Lambda < 0$. Since $A < 0$, the function

$$\varphi(a) := Aa - \frac{C}{2a^2}$$

---

[4]The Einstein static solution $a(t) \equiv \Lambda^{-1/2}$ solves the Friedmann equation Eq. (21) for $k = 1$ and $\rho = \Lambda c^2/(4\pi G)$.

[5]For the time interval $(0, \tau)$, when radiation dominates over matter, the term D/a^2 with constant $D > 0$ is added to the right-hand side of Eq. (26).

is negative and it attains its unique maximum on the interval $(0, \infty)$ at the point

$$a_{\max} = \sqrt[3]{\frac{C}{-A}} > 0.$$

Setting $K := \varphi(a_{\max})$, we deduce by Eq. (27) that

$$\ddot{a}(t) \leq K < 0 \tag{28}$$

for all $t > \tau$ such that $a(t) > 0$, i.e., $a = a(t)$ is strictly concave. By integration we obtain that

$$\dot{a}(t) - \dot{a}(\tau) = \int_\tau^t \ddot{a}(s)\,\mathrm{d}s \leq K(t - \tau) < 0. \tag{29}$$

Since $\dot{a}(\tau)$ and $K\tau$ are fixed numbers and the constant K is negative, we get $\dot{a}(t) < Kt + \text{const}$. By the continuity of $\dot{a}$ and Eq. (22) there exists $t_1 > \tau$ such that

$$\dot{a}(t_1) = 0.$$

Therefore, we always divide by zero in Eq. (24) when $\Lambda < 0$.

2) The well-known case $\Lambda = 0$ also produces division by zero in Eq. (24) when the density $\rho = \rho(t)$ is larger than the so-called critical density $\rho_{\mathrm{crit}}(t) = 3H^2(t)/(8\pi G)$, see e.g. [33, p. 285], [61].

3) Finally, let $\Lambda > 0$. The right-hand side of Eq. (26),

$$F(a) = Aa^2 + B + \frac{C}{a}, \quad a \in (0, \infty),$$

is strictly convex, since its second derivative $F''(a) = 2A + 2C/a^3$ is positive for $a > 0$. From the equation $F'(a) = 2Aa - C/a^2 = 0$ we find that F attains its unique minimum at the point

$$a_{\min} = \sqrt[3]{\frac{C}{2A}} > 0.$$

Now let $k = 1$ and $F(a_{\min}) < 0$. Then there exist two roots $a_1 < a_2$ such that $F(a_1) = F(a_2) = 0$ and F is negative on the interval (a_1, a_2). So let the initial condition $a(\tau)$ satisfy the inequalities $0 < a(\tau) < a_1$. Then F is positive on the interval $(0, a_1)$. Set

$$K := Aa_1 - \frac{C}{2a_1^2}. \tag{30}$$

Since $0 < a_1 < a_{\min}$, we obtain by Eq. (27) that

$$\ddot{a}(t) = Aa(t) - \frac{C}{2a^2(t)} \leq K < Aa_{\min} - \frac{C}{2a_{\min}^2} = 0$$

for all $t > \tau$ such that $a(t) > 0$. Hence, Eq. (28) holds with the constant K given by Eq. (30). From Eq. (29) we again obtain the existence of a time instant $t_2 > \tau$ such that

$$\dot{a}(t_2) = 0 \qquad (\text{and } a(t_2) = a_1).$$

Therefore, the cosmological density parameters are not well defined due to the division by zero in Eq. (24). We also see that their names were not appropriately chosen. For instance, if $k \neq 0$ then the curvature parameters $\Omega_k(t_1)$ and $\Omega_k(t_2)$ approach $\pm\infty$ by Eq. (24) even though nothing dramatic happens.

6. The proclaimed amount of dark matter is over-estimated

According to the standard cosmological model [52], our universe contains more dark matter than ordinary baryonic matter (see Fig. 3) and

$$\text{the ratio of masses of dark matter to baryonic matter} \approx \mathbf{6 : 1}. \qquad (31)$$

The amount of baryonic matter is estimated by a luminous matter [67, p. 74]. The cosmological parameters Eq. (24) are searched so that the solution of Eq. (23) is as close as possible to the measured data.
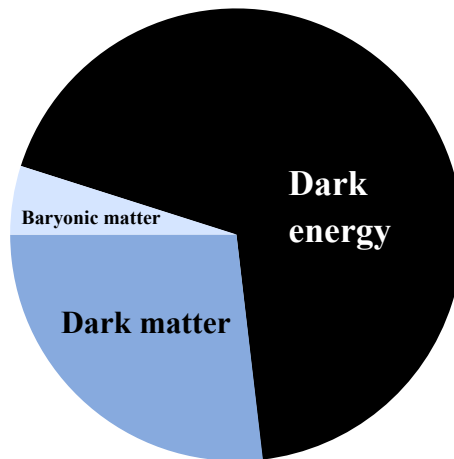

Fig. 3 *Results of the Planck satellite [52] are interpreted in such a way that our universe consists of about 6 times more dark matter than ordinary baryonic matter. However, they are based on the normalized Friedmann equation (23), which was derived using excessive extrapolations by many orders of magnitude.*

In [31], we presented 10 counterarguments showing that such a claimed amount of dark matter Eq. (31) can be a result of vast overestimation and does not conform to reality (see also [39] and references therein). Some of these counterarguments can be convincingly verified even by simple hand calculations. Here we will, therefore, briefly mention only a few main arguments.

The terms dark matter and dark energy from Fig. 3 are inconsistent, i.e., they are not on the same meaning level. Energy is consistent with the term mass through the relation $E = mc^2$. In this case, the physical quantities energy and mass are real numbers with appropriate physical dimensions, while matter is neither a real number nor a physical quantity.

The cosmological parameters Eq. (24) corresponding to the present time t_0 were determined by the three seemingly independent methods of Baryonic Acoustic Oscillations (BAO), Cosmic Microwave Background Radiation[6] (CMB), and Supernovae type Ia explosions (SNe), see Fig. 4. However, these methods are not

---

[6]For a trustworthy criticism of this method we refer to [66].

independent, since the searched cosmological parameters Eq. (24) are supposed to satisfy the same normalized Friedmann equation Eq. (23) in all three methods. Moreover, to extrapolate Einstein's equations from the Solar system to the whole universe, which is at least 15 orders of magnitude larger, is questionable, see [38]. In truth, it is more likely that the measured data just indicate that the extrapolation is wrong, since it requires one to introduce some exotic dark matter and dark energy.
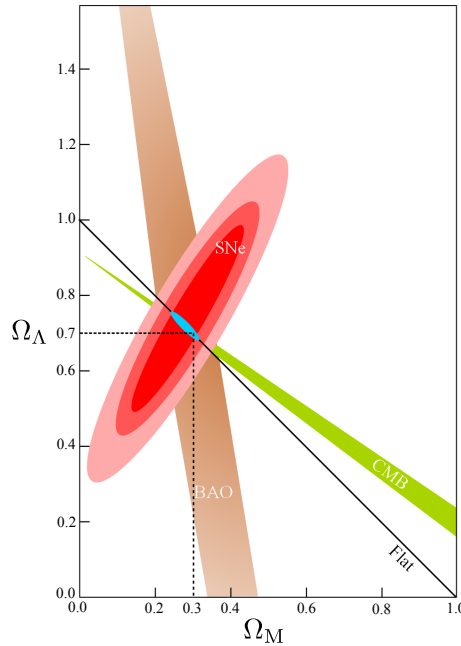

Fig. 4 *Admissible values of cosmological parameters, obtained by three different methods: BAO, CMB, and SNe, intersect in a small region containing cosmological parameters $\Omega_M \approx 0.3$ and $\Omega_\Lambda \approx 0.7$.*

At the end of the 20th century (when Perlmutter et al. published their famous paper [50]) it was thought that red dwarfs of the spectral class M form only 3 % of the total number of stars, see [3, p. 93]. Nevertheless, the Gaia satellite estimated that red dwarfs are in the vast majority — about 75 %. This large portion essentially contributes to invisible baryonic matter.

Taking into account relativistic effects of high velocities, gravitational redshift, gravitational lensing in a curved space, decreasing Hubble parameter, intergalactic baryonic matter, dynamical friction, gravitational aberration, etc., we showed in [33, Chaps. 7–9] that the proclaimed ratio Eq. (31) can be essentially reduced by means of actual data.

Einstein's equations (15) on maximally symmetric space manifolds imply the Friedmann equation (21). This is a mathematical implication, since no approximations are made, see [34] for details. Experiments based on the Friedmann equation imply the existence of a 6 times larger amount of dark matter than bary-

onic matter. Since it appears (see [31]) that this ratio is far from reality, Einstein's equations cannot describe it well. For instance, the perfect spiral shape of galaxies (see Fig. 5) indicates that there is not 6× more gravitationally interacting dark matter than ordinary baryonic matter inside galaxies.

Fig. 5 *Spiral galaxies could not have such a large symmetry if there were to be six times more uniformly distributed dark matter than structured baryonic matter.*

7. Dark energy mystery

By the scientific results of the Planck satellite [52], our universe is composed of about 68 % of some mysterious dark energy, i.e., the present value $\Omega_\Lambda = 0.68$ in Eq. (24). Nevertheless, this quantity was again obtained from the ΛCDM cosmological model which is based on excessive extrapolations [38].

For the luminosity distance of supernovae type Ia explosions, Perlmutter et al. in [50, p. 566] and Riess et al. in [54, p. 1021] used the following formula which was taken from [12, p. 511] (see also [35] for its detailed derivation)

$$d_{\mathrm{L}}(z) = \frac{c(1+z)}{H_0\sqrt{|\Omega_k|}} \mathrm{sinn}\left(\sqrt{|\Omega_k|}\int_0^z \frac{\mathrm{d}\overline{z}}{\sqrt{(1+\overline{z})^2(1+\Omega_{\mathrm{M}}\overline{z}) - \overline{z}(2+\overline{z})\Omega_\Lambda}}\right), \quad (32)$$

where z is the corresponding redshift, sinn is defined by Eq. (20), Ω_{M}, Ω_Λ and Ω_k are values of cosmological parameters Eq. (24) at the present time t_0, and

$$H_0 = H(t_0) \quad (33)$$

is the *Hubble constant*. The distance d_{L} thus essentially depends on the fact whether Einstein's equations on cosmological distances sufficiently well approximate reality,

since the Friedmann equation Eq. (23) is a mathematical consequence of Eq. (15) for a homogeneous and isotropic universe.

At the end of the 20th century, cosmologists believed that the expansion function $a = a(t)$ is concave everywhere, i.e., $\dot{a}$ is a decreasing function of time, since the expansion of the universe is slowed down by an attractive gravitational force. In 1998–1999, the Supernova Cosmology Project and the High-z Supernova Search teams focused on supernovae at large distances corresponding to redshifts of 0.2 to 1. They independently discovered that type Ia supernovae have up to $15\,\%$ lower intensity (see [51], [54]) than they should have if the expansion of the universe were to be decelerating. But this means that the light of a supernova propagates into a larger volume than if the universe expansion slowed down only by gravity. To explain this paradox, it was necessary to introduce, in addition to dark matter, *dark energy* that on the contrary accelerates the expansion of the universe. Thus, it was found that the derivative $\dot{a} = \dot{a}(t)$ is increasing (i.e., a is strictly convex) in the time interval of about the last five billion years, which corresponds approximately to the redshift $0 \leq z \leq 0.5$.

The method SNe (see Fig. 4) treats type Ia supernovae as standard candles. However, they cannot be considered as standard candles due to the possible large extinction of light from the supernova. This essentially depends on its location in the host galaxy, if it is at the edge of a galaxy or in the middle completely surrounded by galactic gas and dust. It also depends on the direction of supernova rotational axis. In this way we may receive several orders of magnitude weaker light.

Finally, the main argument against the proposed amount of dark energy is the 120-order-of-magnitude discrepancy between the measured and theoretically derived density of vacuum energy (see [2]). From this it is evident that the standard cosmological model, which is a direct mathematical consequence of Einstein's equations Eq. (15), does not approximate reality well.

8.   Mercury's perihelion shift revisited

Classical tests of the theory of general relativity, such as bending of light, Mercury's perihelion shift, gravitational redshift, and also Shapiro's fourth test of general relativity (see e.g. [28], [44], [59]) are based on verifications of very simple algebraic formulae (cf. e.g. Eq. (37) below) derived by various simplifications and approximations from the Schwarzschild solution Eq. (10) without any guaranteed error estimates. Nevertheless, we cannot test the validity of Einstein's equations Eq. (1) by means of the Schwarzschild solution. This could be used only to disprove their validity (more precisely, to disprove their good approximation properties of reality). Analogously, good approximation properties of the Laplace equation $\Delta u = 0$ cannot be verified by testing its linear solution $u(x_1, x_2, x_3) = x_1 + x_2 + x_3$, since there exist infinitely many equations having the same solution, e.g. $\Delta u + \partial^n u/\partial x_1^n = 0$ for any integer $n \geq 2$. Thus the equation $\Delta u = 0$ should be tested for all its solutions and not only one solution. Similarly, there exist many other equations than Eq. (1) having the solution Eq. (10), e.g., $R_{\mu\nu} + n(g_{11} - r/(r - S)) = 0$ for any integer $n \geq 1$ due to Eq. (8).

In the current astrophysical community, it is generally accepted that the additional relativistic perihelion shift of Mercury is

$$E = 43'' \text{ per century} \tag{34}$$

and that it is the difference between its observed perihelion shift O caused by other planets (see Fig. 6) and the one C calculated by Newtonian mechanics with infinite speed of gravitational interaction, i.e.,

$$E = O - C. \tag{35}$$

However, this is an ill-conditioned problem due to the subtraction of two quite inexact numbers of almost equal magnitude [7]. Moreover, the quantities O and C are not uniquely defined.
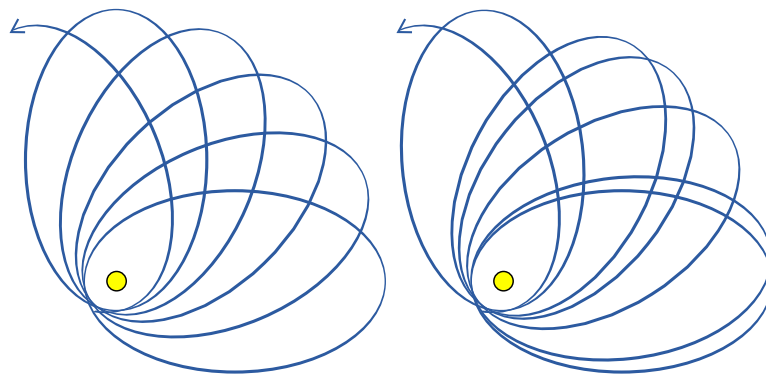
Fig. 6 *An idealized uniform perihelion shift of Mercury in the direction of circulation is shown on the left. For clarity, a very high artificial eccentricity $e = 0.8$ is chosen. On the right is schematically depicted an irregular perihelion shift caused by the gravitational tug of other planets.*

There are many ways how to obtain C. The analytical solution of the associated N-body problem is unknown and moreover unstable in the Lyapunov sense. By [46], the numerically calculated perihelion in the heliocentric system may increase about $24''$ or decrease about $11''$ per year, cf. Fig. 7 and Eq. (34). So it is not clear how to define the mean value per century. Which 100 years? According to [46, p. 657] and [48],

$$O \approx 575'' \text{ per century} \quad \text{and} \quad C \approx 532'' \text{ per century},$$

but in the literature we can find other values of O and C (see [30]). For instance, in [8] the position of each planet is established by more than 100 parameters which are corrected every few years so that they are consistent with the observed positions of the planets. Thus the value $O - C = 43''$ per century is unconvincing.

Note that the full angle has over a million arc seconds, namely,

$$u = 360 \cdot 3600'' = 1\,296\,000''.$$

Eq. (34) gives less than one arc second per year. Mercury's perihelion separation from the Sun is $r = a(1 - e) = 46 \cdot 10^6$ km, where $e = 0.2056$ is the eccentricity
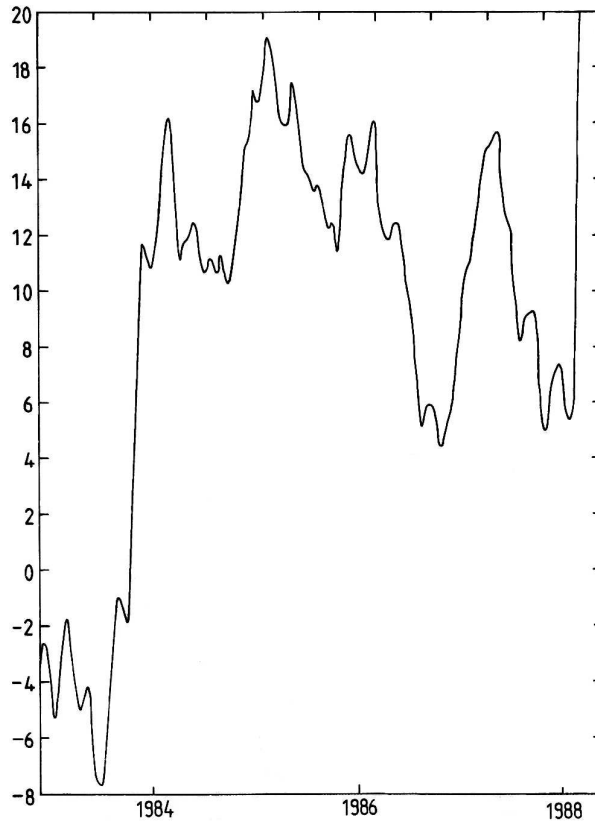
Fig. 7 *The shift of the line of apsides of Mercury's orbit during five years only, calculated numerically from the N-body problem in heliocentric coordinates (adapted from [53]). The graph resembles deterministic chaos. The scale on the horizontal axis is given in years, and on the vertical axis the shift angle is in arc seconds.*

of its elliptic orbit and $a = 57.909 \cdot 10^6$ km the length of its semimajor axis. The Solar system barycenter shifts by about 1000 km every day (see Fig. 8), whereas the additional relativistic perihelion shift of Mercury is by Eq. (34) on average only

$$\frac{2\pi r}{u} \cdot 0.43'' = 96 \text{ km per year.} \tag{36}$$

For comparison, the average orbital speed of Mercury is about 50 km/s. However, the positional data from the Messenger spacecraft were typically taken every 10 minutes during the period 2011–2015, see [48, p. 3]. These values show that Mercury's perihelion shift problem is extremely difficult to solve, see also [30], [64], and [65].

Einstein [16, p. 839] presents the following formula for the relativistic perihelion shift derived by many simplifications and approximations

$$\varepsilon = 24\pi^3 \frac{a^2}{T^2 c^2 (1 - e^2)} = 5.012 \cdot 10^{-7} \text{ rad} \tag{37}$$
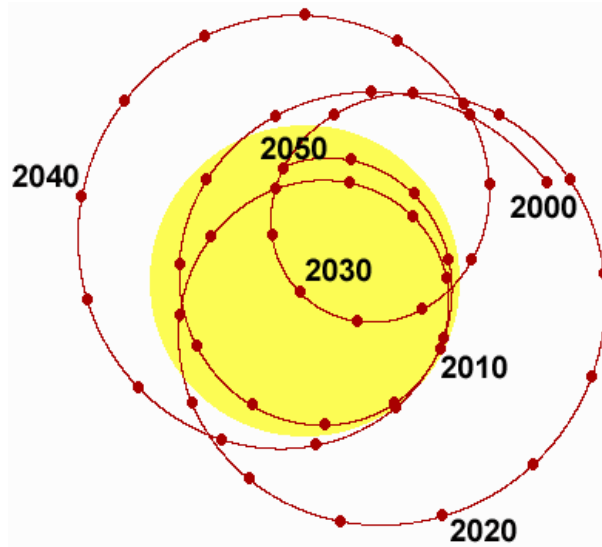
271

Fig. 8 *The trajectory of the Newtonian center of gravity of the Solar system for the period 2000–2050. The center of the Sun (whose diameter is almost 1.4 million km) is at the origin of the heliocentric system. The center of gravity shifts each day by about 1000 km, while the additional relativistic perihelion shift of Mercury is by Eq. (36) on average of only 96 km in a year.*

for one period $T = 7.6005 \cdot 10^6$ s, which yields the idealized value $E = 43''$ per century. Let us emphasize that in [16, p. 832] he did not described the gravitational field around the Sun by Eqs. (8)–(9), but (in our notation) by the equation

$$\Gamma^{\varkappa}_{\mu\nu,\varkappa} - \Gamma^{\lambda}_{\mu\varkappa}\Gamma^{\varkappa}_{\nu\lambda} = 0$$

and, moreover, the Schwarzschild solution Eq. (10) was not known at that time. In [17] he claims (without any proof) that these incomplete equations do not change the proclaimed value Eq. (34). Mercury was replaced by a massless point and the other planets were not taken into account. On the contrary, the quantities O and C from Eq. (35) do include the influence of the other planets. Their effects on the difference $O - C$ do not cancel, because it is a nonlinear problem. Therefore, formula Eq. (34) is not a mathematical consequence of Einstein's equations Eq. (1), since many simplified reasoning and rough approximations were done.

9. Slight violation of the law of conservation of energy

In general relativity the energy-momentum conservation is true only locally, which is expressed in the covariant divergence form as

$$T^{\mu\nu}_{;\nu} := \frac{\partial T^{\mu\nu}}{\partial x^\nu} + \Gamma^{\mu}_{\lambda\nu}T^{\lambda\nu} + \Gamma^{\nu}_{\lambda\nu}T^{\mu\lambda} = 0, \tag{38}$$

see e.g. [24, p. 103], [44, p. 146]. However, in [33] we presented 10 independent observational arguments showing that the Solar system slowly expands. For instance, the mean recession speed of the Earth from the Sun is about 5 m/yr (see [37]) which cannot be explained by the loss of solar mass, or the solar wind or tidal forces. This speed guarantees almost constant influx of solar energy over the past 3.5 Gyr.

The measured recession speed of the Moon from the Earth is 3.84 cm/yr while tidal forces can explain only one half of this value (see [15]). The corresponding remainder is by [33, p. 187] equal to $0.67H_0$, where H_0 is the Hubble constant Eq. (33).

Mars, whose current mean temperature is $-63\,^\circ$C, must have been closer to the Sun (see [29], [42, p. 88]) to have had liquid water on its surface ≈ 3.5 Gyr ago. At that time the luminosity of the Sun was only 75 % of its present value. Thus the greenhouse effect on Mars could hardly increase the mean temperature up to $0\,^\circ$C. For comparison, note that the present greenhouse effect of Earth's atmosphere is only $29\,^\circ$C, see [33, p. 174]. These and several other examples indicate that the law of conservation of energy is slightly violated, since the Solar system is sufficiently isolated from the gravitational influence of nearby stars. By [37] the expansion rate of the Solar system is comparable to H_0. The Hubble constant is thus an important parameter in the context of the Anthropic principle [29].

Slight violation of the laws of conservation of energy and of momentum in the static spacetime can easily explain a wide range of puzzles such as the faint young Sun paradox, the formation of Neptune and Uranus closer to the Sun, the existence of rivers on Mars, the paradox of tidal forces of the Moon, the paradox of the large orbital angular momentum of the Moon and Triton, migration of planets, the slow rotation of Mercury, the absence of its moons [33], etc.

In [33] we also show that galaxies themselves slightly expand. For instance, by [6] and [62] galaxies at cosmological distances have on average more stars per unit volume when compared with the present situation. According to [22], superdense galaxies were quite common in early universe with redshift $z > 1.5$, while at present they are quite rare. Paper [63] also suggests that early galaxies were smaller and denser just after their formation. By [56] the measured stellar mass density in galaxies with $z \leq 3$ is up to 7.9 times higher than for galaxies in our neighborhood. The mass density of some galaxies for $z > 1$ is even comparable with the density of globular clusters (see [9]).

The above arguments support the conjecture that the law of conservation of energy in the static spacetime is slightly violated due to the observed slow expansion of the Solar system and spiral galaxies, and also their clusters. By the theorem of Emmy Noether the energy of each isolated system is conserved if it possesses symmetry with respect to time translations. However, such symmetry is not true for spiraling trajectories.

The angular momentum is also not conserved, see e.g. the recent proceedings [47] for the galactic angular momentum paradox: *How is it possible that spiral galaxies (originating from small random fluctuations in a hot homogeneous and isotropic universe) rotate so fast?* Their orbital speed v satisfies the Tully-Fisher relation $v^4 \sim M$, where M is the mass of a spiral galaxy [43].

10. Scale non-invariance

First, it is necessary to emphasize that no equation of mathematical physics describes reality absolutely exactly on any scale. The reason is that the laws of physics are not unchanged under a change of scale, in general. For instance, the trivial relation for the distance $s = vt$ is scale invariant in the Euclidean space, but in reality it is not scale invariant, since the velocity v is always less than c. We cannot apply it on very small scales due to the Heisenberg uncertainty principle and on very large scales due to the expansion of the universe. Thus also Einstein's equations do not trustworthy describe phenomena at atomic level (see also Section 3) or an extreme state just after Big Bang when quantum effect played an important role.

Second, it is evident that gravity works on different scales in different ways. For instance, planetary systems, globular clusters, spiral galaxies (with 2, 3, or 4 arms), galaxy clusters, and large-scale structures of sheets and filaments consisting of galaxy superclusters have completely different shapes. All these entities are governed by gravity, but it is hard to imagine that all of them would be described only by Eq. (15). For instance, its static solution Eq. (17) is not scale invariant, since it contains the fixed physical constants Λ, c, and G through relation Eq. (12), where the scale is given by the Schwarzschild radius S.

Third, in [38] we present other examples showing why excessive extrapolations of Einstein's equations to cosmological distances are questionable. These extrapolations indicate that the proclaimed dark matter and dark energy arise mostly due to modeling errors. When the curvature index $k = 1$, then the corresponding space manifold is $\mathbb{S}^3(t)$. Since it is bounded, the scale invariance cannot hold.

Fourth, the scale non-invariance in time follows from the previous section. The present state of our universe depends on its history, whereas the first order ordinary differential Friedmann equation Eq. (21) is reversible in time, i.e., its solution for $t > t_0$ depends only on the value of the expansion function at the present time t_0 and it is independent of its history before t_0.

11. Other arguments

The age of the universe was derived from the ΛCDM model up to four significant digits

$$t_0 = 13.79 \text{ Gyr} \tag{39}$$

using the backward integration of the Friedmann equation (26) and the present value of the Hubble constant H_0. Nevertheless, from such a simple equation we should not make any categorical conclusions about the real age of the universe, since it was derived from Einstein's equations by excessive extrapolations to cosmological scales. For instance, by [13] the oldest known star HD 140283 was formed 14.46±0.8 Gyr ago (cf. Eq. (39)). Bond et al. [5] improved this estimate to 14.46 ± 0.31 Gyr, which is in conflict with Eq. (39). The reason is that stars are born by gravitational collapse of very cold gas (about 10 K) which was not available shortly after the Big Bang. Moreover, it is very probable that there are older stars in the whole Universe than HD 140283 from the solar neighborhood.

In 2016, the Planck Collaboration stated that $H_0 = 66.93 \pm 0.62$ km s^{-1}Mpc^{-1}. This value is based on the standard cosmological model (i.e. Einstein's equations), while the Gaia and Hubble Space Telescope measurements of Cepheids and RR Lyrae yield $H_0 = 73.52 \pm 1.62$ km s^{-1}Mpc^{-1}, see [55]. We again get a contradiction between theory and observations.

In [32] we prove the following theorem showing that Einstein's equations should not be applied to galactic or cosmological scales. Consider a fixed nonrotating ball in vacuum with mass $M > 0$ and with a spherically symmetric mass distribution. The Euclidean volume of the spherical shell $r_0 \leq r \leq r_1$ illustrated in Fig. 2 equals $V = \frac{4}{3}\pi(r_1^3 - r_0^3)$. By Birkhoff's theorem [4] the space outside the mass ball is described by the exterior Schwarzschild metric Eq. (10). Thus, for the static case the proper (relativistic) volume of the spherical shell is by the Fubini theorem equal to

$$\tilde{V} = \int_{r_0}^{r_1} r^2 \sqrt{\frac{r}{r-S}}\,\mathrm{d}r \cdot \int_0^{2\pi}\left(\int_0^\pi \sin\theta\,\mathrm{d}\theta\right)\mathrm{d}\varphi = 4\pi \int_{r_0}^{r_1} r^2 \sqrt{\frac{r}{r-S}}\mathrm{d}r.$$

Theorem 2. *Let $M > 0$ and $r_0 > S$ be fixed. Then*

$$\tilde{V} - V \to \infty \quad \text{for } r_1 \to \infty.$$

This theorem can be applied e.g. to an imperceptible pinhead, since the mass $M > 0$ can be arbitrarily small which yields quite absurd result.

The right-hand side of Einstein's equations should contain the speed of gravity instead of the speed of electromagnetic interaction, even though it seems (see [1]) that these speeds are the same under normal conditions.

Einstein's equations do not contain delays (in time variables) corresponding to the finite speed of gravity. This does not allow to treat properly aberration effects. The actual angle of gravitational aberration has to be necessarily positive, since the zero aberration angle would contradict causality [33]. In fact, the causality principle should be prior to the law of conservation of energy.

In the framework of general relativity Steven Carlip in [10] derived that the gravitational aberration angle of a body with speed v is bounded from above by the fraction v^3/c^3, while the angle of light aberration is approximately equal to v/c. However, he assumed that the laws of energy and momentum conservation hold exactly. Since electromagnetic and gravitational interaction have probably the same speed [1], the corresponding aberration angles should have the same size.

It is not known whether close binary systems producing gravitational waves are really described by Eq. (1) or (15). Einstein [20] used several approximations that led to a nonhomogeneous partial differential equation with the d'Alembert operator for a plane gravitational wave far away from its source. Therefore, recent detections of gravitational waves do not confirm that Einstein's equations describe reality well.

Appendices

Appendix A: Calculation of the Christoffel symbols

Let the assumptions (a), (b), (c), and (d) from Section 2 be valid. Entries of the Ricci tensor (see Eq. (49) below) are defined by means of the Christoffel symbols. In the

covariant form (i.e. only with lower indices) the *Christoffel symbols of the first kind* are defined as follows

$$\Gamma_{\mu\nu\varkappa} = \frac{1}{2}(g_{\mu\nu,\varkappa} + g_{\varkappa\mu,\nu} - g_{\nu\varkappa,\mu}), \quad \mu, \nu, \varkappa = 0, 1, 2, 3, \tag{40}$$

where $g_{\mu\nu,\varkappa} = \partial g_{\mu\nu}/\partial x^{\varkappa}$. This is altogether $4 \times 4 \times 4 = 64$ entries. However, since the metric tensor is symmetric, we get by Eq. (40) the following symmetry in the last two indices

$$\Gamma_{\mu\nu\varkappa} = \frac{1}{2}(g_{\mu\varkappa,\nu} + g_{\nu\mu,\varkappa} - g_{\varkappa\nu,\mu}) = \Gamma_{\mu\varkappa\nu}, \tag{41}$$

i.e., there are only $4 \times 10 = 40$ independent Christoffel symbols. From Eq. (40) also have $g_{\mu\nu,\varkappa} = \Gamma_{\mu\nu\varkappa} + \Gamma_{\nu\mu\varkappa}$.

Under the coordinate transformation $\sim: (t, r, \varphi, \theta) \mapsto (-t, r, \varphi, \theta)$ the metric components change as follows

$$\tilde{g}_{\mu 0} = -g_{\mu 0} \quad \text{for } \mu \neq 0,$$

but they should be the same. Therefore,

$$g_{\mu 0} = 0 \quad \text{for } \mu \neq 0.$$

Similarly, the coordinate transformations

$$(t, r, \varphi, \theta) \mapsto (t, r, -\varphi, \theta) \quad \text{and} \quad (t, r, \varphi, \theta) \mapsto (t, r, \varphi, -\theta)$$

yield $g_{\mu 2} = 0$ for $\mu \neq 2$ and $g_{\mu 3} = 0$ for $\mu \neq 3$, respectively. Consequently, from the symmetry of the metric tensor we get

$$g_{\mu\nu} = 0 \quad \text{for } \mu \neq \nu$$

and thus the metric tensor is diagonal. The corresponding four diagonal entries are independent of time coordinate t, because the gravitational field is static.

Since our problem is spherically symmetric, the metric tensor is of the form

$$g_{\mu\mu} = \mathrm{diag}\big(-A(r), B(r), r^2 \sin^2 \theta, r^2\big). \tag{42}$$

We shall look for the unknown functions $A = A(r)$ and $B = B(r)$ which satisfy

$$A(r) \to 1 \quad \text{and} \quad B(r) \to 1 \quad \text{for } r \to \infty, \tag{43}$$

since the spacetime is asymptotically flat.

For $\mu = \nu$ we find by (40) that

$$\Gamma_{\mu\mu\varkappa} = \frac{1}{2}(g_{\mu\mu,\varkappa} + g_{\varkappa\mu,\mu} - g_{\mu\varkappa,\mu}) = \frac{1}{2}g_{\mu\mu,\varkappa}.$$

From this and Eq. (40) by differentiating with respect to t, r, φ, θ we get

$$\Gamma_{001} = -\frac{1}{2}A', \ \Gamma_{111} = \frac{1}{2}B', \ \Gamma_{221} = r \sin^2 \theta, \ \Gamma_{223} = r^2 \sin\theta \cos\theta, \ \Gamma_{331} = r, \tag{44}$$

where the prime indicates the differentiation along r, and

$$\Gamma_{\mu\mu\varkappa} = 0$$

for the other cases. Moreover, by Eq. (40) and (42) we obtain

$$\Gamma_{100} = -\frac{1}{2}g_{00,1} = \frac{1}{2}A',$$

$$\Gamma_{122} = -\frac{1}{2}g_{22,1} = -r\sin^2\theta,$$

$$\Gamma_{133} = -\frac{1}{2}g_{33,1} = -r,$$

$$\Gamma_{322} = -\frac{1}{2}g_{22,3} = -r^2\sin\theta\cos\theta,$$

(45)

and the other Christoffel symbols are zero.

To get once contravariant and twice covariant Christoffel symbols (i.e. with one upper and two lower indices) that appear in Eq. (5), we use the following relation (cf. also [44, p. 340])

$$\Gamma^\mu_{\ \nu\varkappa} = g^{\mu\lambda}\Gamma_{\lambda\nu\varkappa}$$

(46)

with summation over $\lambda = 0, 1, 2, 3$, where $\Gamma_{\lambda\nu\varkappa}$ are defined by Eq. (40),

$$g^{\mu\mu} = \mathrm{diag}\Big(-\frac{1}{A(r)}, \frac{1}{B(r)}, \frac{1}{r^2\sin^2\theta}, \frac{1}{r^2}\Big)$$

(47)

is the inverse matrix to $g_{\mu\mu}$ for $A(r) \neq 0 \neq B(r)$ and $0 < \theta < \pi$. Since $g^{\mu\mu}$ is diagonal and $\Gamma^\mu_{\ \nu\varkappa} = \Gamma^\mu_{\ \varkappa\nu}$, we get by Eqs. (44), (45), (46), and (47) that

$$\Gamma^0_{\ 01} = g^{00}\Gamma_{001} = \frac{A'}{2A},$$

$$\Gamma^1_{\ 00} = g^{11}\Gamma_{100} = \frac{A'}{2B},$$

$$\Gamma^1_{\ 11} = g^{11}\Gamma_{111} = \frac{B'}{2B},$$

$$\Gamma^1_{\ 22} = g^{11}\Gamma_{122} = -\frac{r\sin^2\theta}{B},$$

$$\Gamma^1_{\ 33} = g^{11}\Gamma_{133} = -\frac{r}{B},$$

$$\Gamma^2_{\ 12} = g^{22}\Gamma_{221} = \frac{1}{r^2\sin^2\theta}r\sin^2\theta = \frac{1}{r},$$

$$\Gamma^2_{\ 23} = g^{22}\Gamma_{223} = \frac{1}{r^2\sin^2\theta}r^2\sin\theta\cos\theta = \cot\theta,$$

$$\Gamma^3_{\ 13} = g^{33}\Gamma_{331} = \frac{1}{r^2}r = \frac{1}{r},$$

$$\Gamma^3_{\ 22} = g^{33}\Gamma_{322} = -\sin\theta\cos\theta,$$

(48)

and the other Christoffel symbols are zero.

Appendix B: Calculation of the Ricci tensor

First recall the definition of the Ricci tensor from Eq. (9),

$$R_{\mu\nu} = R_{\nu\mu} = \Gamma^\varkappa_{\ \mu\nu,\varkappa} - \Gamma^\varkappa_{\ \mu\varkappa,\nu} + \Gamma^\lambda_{\ \mu\nu}\Gamma^\varkappa_{\ \lambda\varkappa} - \Gamma^\lambda_{\ \mu\varkappa}\Gamma^\varkappa_{\ \nu\lambda}.$$

(49)

277

From this and Eq. (8) we have

$$R_{00} = \Gamma^{\varkappa}{}_{00,\varkappa} - \Gamma^{\varkappa}{}_{0\varkappa,0} + \Gamma^{\lambda}{}_{00}\Gamma^{\varkappa}{}_{\lambda\varkappa} - \Gamma^{\lambda}{}_{0\varkappa}\Gamma^{\varkappa}{}_{0\lambda} = \Gamma^{1}{}_{00,1} + \Gamma^{1}{}_{00}\Gamma^{\varkappa}{}_{1\varkappa} - 2\Gamma^{1}{}_{00}\Gamma^{0}{}_{01}$$

$$= \frac{A''B - A'B'}{2B^2} + \frac{A'}{2B}\left(\frac{A'}{2A} + \frac{B'}{2B} + \frac{2}{r}\right) - 2\frac{A'}{2B}\frac{A'}{2A}$$

$$= \frac{A''}{2B} - \frac{A'}{4B}\left(\frac{A'}{A} + \frac{B'}{B}\right) + \frac{A'}{rB} = 0. \tag{50}$$

Similarly, we obtain

$$R_{11} = -\Gamma^{0}{}_{10,1} - \Gamma^{2}{}_{12,1} - \Gamma^{3}{}_{13,1} + \Gamma^{1}{}_{11}\Gamma^{\varkappa}{}_{1\varkappa} - (\Gamma^{\varkappa}{}_{1\varkappa})^2$$

$$= -\frac{A''}{2A} + \frac{A'}{4A}\left(\frac{A'}{A} + \frac{B'}{B}\right) + \frac{B'}{rB} = 0, \tag{51}$$

$$R_{33} = \Gamma^{1}{}_{33,1} - \Gamma^{2}{}_{32,3} + \Gamma^{1}{}_{33}(\Gamma^{0}{}_{01} + \Gamma^{1}{}_{11} + \Gamma^{2}{}_{21} + \Gamma^{3}{}_{31}) - 2\Gamma^{3}{}_{31}\Gamma^{1}{}_{33}$$

$$= -\frac{1}{B} + \frac{1}{\sin^2\theta} - \frac{r}{2B}\left(\frac{A'}{A} - \frac{B'}{B}\right) = 0, \tag{52}$$

and

$$R_{22} = R_{33}\sin^2\theta = 0. \tag{53}$$

Multiplying Eq. (50) by B/A and summing with Eq. (51), we obtain

$$A'B + AB' = 0$$

which means that AB is constant. From boundary conditions Eq. (43) we find that this constant is

$$AB = 1.$$

Substituting $B = 1/A$ into Eq. (52) for $\theta = \pi/2$ (the plane of symmetry), we obtain $A + rA' = 1$ which yields

$$\frac{\mathrm{d}(rA)}{\mathrm{d}r} = 1.$$

By integration we get

$$rA = r - S,$$

where the constant S has to be chosen so that Eq. (12) holds (see e.g. [24, p. 121] for details). Hence,

$$A(r) = \frac{r - S}{r} \quad \text{and} \quad B(r) = \frac{r}{r - S}, \tag{54}$$

i.e., the relation Eq. (10) is true.

Appendix C: Calculation of the Schwarzschild-de Sitter metric

The procedure to get the metric tensor satisfying Eq. (17) is similar to the case $\Lambda = 0$ investigated above. According to [11, p. 195], an exterior metric associated to a ball with spherically symmetric mass distribution can be described by the diagonal metric tensor (cf. Eq. (42))

$$g_{\mu\mu} = \mathrm{diag}\left(-\mathrm{e}^{2\alpha(r)}, \mathrm{e}^{2\beta(r)}, r^2\sin^2\theta, r^2\right). \tag{55}$$

We shall look for the unknown functions $\alpha = \alpha(r)$ and $\beta = \beta(r)$ so that Eq. (17) is satisfied. By to [11, p. 195] the entries of the Ricci tensors are

$$R_{00} = e^{2(\alpha-\beta)}\Big(\alpha'' + (\alpha')^2 - \alpha'\beta' + \frac{2\alpha'}{r}\Big),$$

$$R_{11} = -\alpha'' - (\alpha')^2 + \alpha'\beta' + \frac{2\beta'}{r}, \tag{56}$$

$$R_{33} = e^{-2\beta}(r(\beta' - \alpha') - 1) + 1,$$

and we again have $R_{22} = R_{33}\sin^2\theta = 0$ as in Eq. (53). Multiplying the equation $R_{00} = \Lambda g_{00} = -\Lambda e^{2\alpha}$ by $e^{-2(\alpha-\beta)}$, we obtain

$$\alpha'' + (\alpha')^2 - \alpha'\beta' + \frac{2\alpha'}{r} = -\Lambda e^{2\beta}.$$

Summing this with Eq. (56), we get by Eq. (17) and (55) that

$$\frac{2(\alpha' + \beta')}{r} = 0.$$

This means that $\alpha + \beta$ is a constant, which can be chosen zero (see [11, p. 196]). Hence,

$$\alpha = -\beta. \tag{57}$$

Substituting this into the equation $R_{33} = \Lambda g_{33}$, we find by Eq. (55) and (56) that

$$1 - \Lambda r^2 = e^{2\alpha}(2r\alpha' + 1) = \frac{\partial}{\partial r}\big(e^{2\alpha}r\big).$$

Therefore,

$$re^{2\alpha} = r - \frac{\Lambda r^3}{3} + C$$

for some integration constant C, i.e.

$$e^{2\alpha} = 1 - \frac{C}{r} - \frac{\Lambda r^2}{3} > 0 \tag{58}$$

keeping in mind the discussion after formula Eq. (19). Requiring that the resulting metric changes into Eq. (10) for $\Lambda \to 0$, we see that the constant C should be equal to the Schwarzschild radius S given by (12). Then by Eqs. (55), (57), and (58) the Schwarzschild metric with generally nonzero cosmological constant is

$$g_{\mu\mu} = \mathrm{diag}\Big(-\Big(\frac{r-S}{r} - \frac{\Lambda r^2}{3}\Big), \Big(\frac{r-S}{r} - \frac{\Lambda r^2}{3}\Big)^{-1}, r^2\sin^2\theta, r^2\Big). \tag{59}$$

Acknowledgement

References

[1] ABBOTT B.P. et al., GW170817: Observation of gravitational waves from a binary neutron star inspiral. *Phys. Rev. Lett.* 2017, 119, Article ID 161101, doi: 10.1103/PhysRevLett.119.161101.

[2] ADLER J.R., CASEY B., JACOB O.C. Vacuum catastrophe: An elementary exposition of the cosmological constant problem. *Amer. J. Phys.* 1995, 63, pp. 620–626, doi: 10.1119/1.17850.

[3] BINNEY J., MERRIFIELD M. *Galactic astronomy*. Princeton, 1998.

[4] BIRKHOFF G.D. *Relativity and modern physics*. Harvard Univ. Press, Cambridge, Massachusetts, 1923.

[5] BOND H.E. et al. HD 140283: A star in the solar neighborhood that formed shortly after the Big Bang. ArXiv: 1302.3180v1, 2013, pp. 1–19.

[6] BOUWENS R.J. et al. A candidate redshift $z \approx 10$ galaxy and rapid changes in that population at an age of 500 Myr. *Nature* 2011, 469, pp. 504–507, doi: 10.1038/nature09717.

[7] BRANDTS J., KŘÍŽEK M., ZHANG Z. Paradoxes in numerical calculations. *Neural Netw. World* 2016, 26(3), pp. 317–330, doi: 10.14311/NNW.2016.26.018.

[8] BRETAGNON P., FRANCOU G. Planetary theories in rectangular and spherical variables. VSOP 87 solutions. *Astron. Astrophys.* 1988, 202, pp. 309–315.

[9] BUITRAGO F. et al. Shaping massive galaxies: their morphology and kinematics at $z = 1-3$. *Highlights of Spanish Astrophysics VI, Proc. of the IX Sci. Meeting of the Spanish Astronom. Soc.* (ed. M.R. Zapatero et al.), Madrid, 2010, 154–160.

[10] CARLIP S. Aberration and the speed of gravity. *Phys. Lett. A* 2000, 267, pp. 81–87, doi: 10.1016/s0375-9601(00)00101-8.

[11] CARROLL S. *Spacetime and geometry. An introduction to general relativity*. Pearson, Harlow, 2014.

[12] CARROLL S.M., PRESS H.W., TURNER E.L. The cosmological constant. *Annu. Rev. Astron. Astrophys.* 1992, 30, pp. 499–542, doi: 10.1146/annurev.astro.30.1.499.

[13] COWEN R. Nearby star is almost as old as the Universe. *Nature* 2013, January 10, doi: 10.1038/nature.2013.12196.

[14] DE SITTER W. On the relativity of inertia. Remarks concerning Einstein latest hypothesis. *Proc. Kon. Ned. Acad. Wet.* 1917, 19, pp. 1217–1225.

[15] DUMIN Y.V. A new application of the Lunar laser retroreflectors: Searching for the "local" Hubble expansion. *Adv. Space Res.* 2003, 31(11), pp. 2461–2466, doi: 10.1016/S0273-1177(03)00533-7.

[16] EINSTEIN A. Erklärung der Perihelbewegung des Merkur aus der allgemeinen Relativitätstheorie. *Königlich-Preußische Akad. Wiss.* Berlin, 1915, pp. 831–839. Eng. trans. Explanation of the perihelion motion of Mercury from general relativity theory, by R.A. Rydin with comments by A.A. Vankov, pp. 1–34.

[17] EINSTEIN A. Die Feldgleichungen der Gravitation. *Sitzungsber. Preuss. Akad. Wiss.* 1915, 48, pp. 844–847.

[18] EINSTEIN A. The foundation of the general theory of relativity. *Ann. Phys.* 1916, 49, pp. 769–822.

[19] EINSTEIN A. Kosmologische Betrachtungen zur allgemeinen Relativitätstheorie. *Königlich-Preuss. Akad. Wiss.* Berlin, 1917, pp. 142–152. Eng. trans. in *The principle of relativity*. New York: Dover, 1952.

[20] EINSTEIN A. Über Gravitationswellen. *Sitzungsberichte K. Preuss. Akad. Wiss.* 1918, 1, pp. 154–167.

[21] ELLIS H.G. Gravity inside a nonrotating, homogeneous, spherical body. ArXiv: 1203.4750v2, 2012, pp. 1–6.

280

[22] FERRÉ-MATEU A., TRUJILLO I. Superdense massive galaxies in the nearby universe. *Proc. of the XXVII. General Assembly of IAU, S262* (eds. G. Bruzual, S. Charlot), Kluwer, 2010, pp. 331–332.

[23] FLORIDES P.S. A new interior Schwarzschild solution. *Proc. Roy. Soc. London A* 1974, 337, pp. 529–535, doi: `10.1098/rspa.1974.0065`.

[24] FOSTER J., NIGHTINGALE J.D. *A short course in general relativity.* Springer, New York, 1995, doi: `10.1007/978-0-387-27583-3`.

[25] FRIEDMAN A. Über die Krümmung des Raumes. *Z. Phys.* 1922, 10(1), pp. 377–386. Eng. trans. On the curvature of space. *General Relativity and Gravitation* 1999, 31, pp. 1991–2000, doi: `10.1007/BF01332580`.

[26] HLAVÁČEK I., KŘÍŽEK M., MALÝ J. On Galerkin approximations of a quasilinear non-potential elliptic problem of a nonmonotone type. *J. Math. Anal. Appl.* 1994, 184(1), pp. 168–189, doi: `10.1006/jmaa.1994.1192`.

[27] KOTTLER F. Über die physikalischen Grundlagen der Einsteinschen Gravitationstheorie. *Ann. Physik* 1918, 56, pp. 401–462, doi: `10.1002/andp.19183611402`.

[28] KRANIOTIS G.V., WHITEHOUSE S.B. Compact calculation of the perihelion precession of Mercury in general relativity, the cosmological constant and Jacobi's inversion problem. *Class. Quant. Grav.* 2003, 20, pp. 4817–4835, doi: `10.1088/0264-9381/20/22/007`.

[29] KŘÍŽEK M. Dark energy and the anthropic principle. *New Astronomy* 2012, 17(1), pp. 1–7, doi: `10.1016/j.newast.2011.05.003`.

[30] KŘÍŽEK M. Influence of celestial parameters on Mercury's perihelion shift. *Bulg. Astron. J.* 2017, 27, pp. 41–56.

[31] KŘÍŽEK M. Ten arguments against the proclaimed amount of dark matter. *Grav. Cosmol.* 2018, 24(4), pp. 350–359, doi: `10.1134/S020228931804014X`.

[32] KŘÍŽEK M., KŘÍŽEK F. Quantitative properties of the Schwarzschild metric. *Publ. Astron. Soc. Bulg.* 2018, 1, pp. 1–10.

[33] KŘÍŽEK M., KŘÍŽEK F., SOMER L. *Antigravity – its origin and manifestations.* Lambert Acad. Publ., Saarbrücken, 2015.

[34] KŘÍŽEK M., MÉSZÁROS A. On the Friedmann equation for the three-dimensional hyper-sphere. *Proc. Conf. Cosmology on Small Scales 2016, Local Hubble Expansion and Selected Controversies in Cosmology* (eds. M. Křížek, Y.V. Dumin), Inst. of Math., Prague, 2016, pp. 159–178.

[35] KŘÍŽEK M., MÉSZÁROS A. Classification of distances in cosmology. *Proc. Conf. Cosmology on Small Scales 2018, Dark Matter Problem and Selected Controversies in Cosmology* (eds. M. Křížek, Y.V. Dumin), Inst. of Math., Prague, 2018, pp. 92–118.

[36] KŘÍŽEK M., SOMER L. A critique of the standard cosmological model. *Neural Netw. World* 2014, 24(5), pp. 435–461, doi: `10.14311/NNW.2014.24.026`.

[37] KŘÍŽEK M., SOMER L. Manifestations of dark energy in the Solar system. *Gravit. Cosmol.* 2015, 21(1), pp. 59–72, doi: `10.1134/S0202289315010090`.

[38] KŘÍŽEK M., SOMER L. Excessive extrapolations in cosmology. *Gravit. Cosmol.* 2016, 22(3), pp. 270–280, doi: `10.1134/S0202289316030105`.

[39] KROUPA P. The dark matter crisis: Falsification of the current standard model of cosmology. *Publ. Astron. Soc. Australia* 2012, 29, pp. 395–433, doi: `10.1071/as12005`.

[40] LANCZOS C. Über eine stationäre kosmologie im sinne der Einsteinischen Gravitationstheories. *Zeitschr. f. Phys.* 1924, 21, pp. 73–110, doi: `10.1007/bf01328251`.

[41] LANDAU L.D., LIFSHITZ E.M. *The classical theory of fields* (4th revised edition). Pergamon Press Ltd., 1975 (also Izd. Nauka, Moskva, 1973).

[42] MAEDER A., BOUVIER P. Scale invariance, metrical connection and the motions of astronomical bodies. *Astronom. Astrophys.* 1979, 73, pp. 82–89.

[43] MAKAROV D.I., ZAITSEVA N.A., BIZYAEV D.V. Multiparametric Tully-Fisher relation for late type edge-on galaxies. *Proc. Conf. Cosmology on Small Scales 2018, Dark Matter Problem and Selected Controversies in Cosmology* (eds. M. Křížek, Y.V. Dumin), Inst. of Math., Prague, 2018, pp. 75–91.

[44] MISNER C.W., THORNE K.S., WHELLER J.A. *Gravitation*, 20th edition. New York: W.H. Freeman, 1997.

[45] MOORE T.A. *A general relativity workbook*. Univ. Sci. Books, 2013.

[46] NARLIKAR J.V., RANA N.C. Newtonian N-body calculations of the advance of Mercury's perihelion. *Mon. Not. R. Astron. Soc.* 1985, 213, pp. 657–663, doi: 10.1093/mnras/213.3.657.

[47] OBRESCHKOW D. et al. (eds.) *Galactic angular momentum*. Proc. XXXth IAU General Assembly, Focus Meeting 6, Vienna, August, 2018.

[48] PARK R.S. et al. Precession of Mercury's perihelion from ranging to the *MESSENGER* Spacecraft. *Astron. J.* 2017, 153(121), pp. 1–7, doi: 10.3847/1538-3881/aa5be2.

[49] PERLMUTTER S. Supernovae, dark energy, and the accelerating universe. *Physics Today* 2003, 56, April, pp. 53–60, doi: 10.1063/1.1580050.

[50] PERLMUTTER S. et al. Measurements of the cosmological parameters Ω and Λ from the first seven supernovae at $z \geq 0.35$. *Astrophys. J.* 1997, 483, pp. 565–581, doi: 10.1086/304265.

[51] PERLMUTTER S. et al. Measurements of Ω and Λ from 42 high-redshift supernovae. *Astrophys. J.* 1999, 517, pp. 565–586, doi: 10.1086/307221.

[52] PLANCK COLLABORATION, Planck 2013 results, I. Overview of products and scientific results. *Astron. Astrophys.* 2014, 571, A1, pp. 1–48, doi: 10.1051/0004-6361/201321529.

[53] RANA N.C. An investigation of the motions of the node and perihelion of Mercury. *Astron. Astrophys.* 1987, 181, pp. 195–202.

[54] RIESS A.G. et al. Observational evidence from supernovae for an accelerating universe and a cosmological constant. *Astron. J.* 1998, 116(3), pp. 1009–1038, doi: 10.1086/300499.

[55] RIESS A.G. et al. Milky Way Cepheid standards for measuring cosmic distances and application to GAIA DR2: Implications for the Hubble constant. *Astrophys. J.* 2018, 861, Article ID 126, doi: 10.3847/1538-4357/aac82e.

[56] RUDNICK G. et al. Measuring the average evolution of luminous galaxies at $z < 3$: The rest-frame optical luminosity density, spectral energy distribution, and stellar mass density. *Astrophys. J.* 2006, 650, pp. 624–643, doi: 10.1086/507123.

[57] SCHWARZSCHILD K. Über das Gravitationsfeld eines Massenpunktes nach der Einsteinschen Theorie. *Sitzungsber. Preuss. Akad. Wiss.* 1916, pp. 189–196. Eng. trans. On the gravitational field of a point-mass, according to Einstein's theory. *The Abraham Zelmanov Journal* 2008, 1, pp. 10–19.

[58] SCHWARZSCHILD K. Über das Gravitationsfeld einer Kugel aus incompressiebler Flüssigkeit nach der Einsteinschen Theorie. *Sitzungsber. Preuss. Akad. Wiss.* 1916, pp. 424–435. Eng. trans. On the gravitational field of a sphere of incompressible liquid, according to Einstein's theory. *The Abraham Zelmanov Journal* 2008, 1, pp. 20–32.

[59] SHAPIRO I.I. Fourth test of general relativity. *Phys. Rev. Lett.* 1964, 13(26), 789–791, doi: 10.1103/PhysRevLett.13.789.

[60] STEPHANI H. *Relativity: An introduction to special and general relativity*, 3rd edition. Cambridge Univ. Press, Cambridge, 2004.

[61] TOLMAN R.C. *Relativity, thermodynamics, and cosmology*. Clarendon Press, Oxford, 1934; Dover, New York, 1987.

[62] TRUJILLO I. et al. Strong size evolution of the most massive galaxies since $z \sim 2$. *Mon. Not. R. Astron. Soc.* 2007, 382, pp. 109–120, doi: 10.1111/j.1365-2966.2007.12388.x.

[63] VAN DE SANDE J. et al. The stellar velocity dispersion of a compact massive galaxy at $z = 1.80$ using X-shooter confirmation of the evolution in the mass-size and mass-dispersion relations. *Astrophys. J. Lett.* 2011, 736, L9.

[64] VANKOV A.A. General relativity problem of Mercury's perihelion advance revisited. ArXiv: 1008.1811v1, 2010, pp. 1–46.

[65] VANKOV K. *Particle orbits in general relativity: from planetary Solar system to black hole environment.* Lecture Notes, Univ. Grenoble, 2018, pp. 1–75.

[66] VAVRYČUK V. Universe opacity and CMB. *Mon. Not. R. Astron. Soc.* 2018, 478(1), pp. 283–301, doi: 10.1093/mnras/sty974.

[67] WEINBERG S. *Cosmology.* Oxford Univ. Press, 2008.

[68] WEYL H. Über die statischen, kugelsymmetrischen Lösungen von Einsteins "kosmologis- chen" Gravitationsgleichungen. *Phys. Z.* 1919, 20, pp. 31–34.